Wavefield extrapolation in Riemannian coordinates

Paul Sava, Stanford University and Sergey Fomel, Bureau of Economic Geology, UT Austin*

SUMMARY

Riemannian spaces are described by non-orthogonal curvilinear coordinates. We generalize one-way wavefield extrapolation to semi-orthogonal Riemannian coordinate systems, which include, but are not limited to, ray coordinate systems. The result are one-way wavefield extrapolation methods which are not dip-limited, and which can even be used to image overturning waves. Ray coordinate systems can be initiated either from point sources, or from plane waves incident at various angles. Since wavefield propagation happens mostly along the extrapolation direction, we can use inexpensive finite-difference or mixed-domain extrapolators to achieve high angle accuracy. The main applications of our method include imaging of steeply dipping or overturning reflections.

INTRODUCTION

Imaging complex geology is one of the main challenges of today's seismic processing. Of the many seismic imaging methods available, downward continuation (Claerbout, 1985) has proven to be accurate, robust, and capable of handling models with large and sharp velocity variations. Such methods naturally handle the multipathing which occurs in complex geology and provide a band-limited solution to the seismic imaging problem. Furthermore, as computational power increases, such methods are gradually moving into the mainstream of seismic processing. This explains why one-way wave extrapolation has been a subject of extensive theoretical research in the recent years (Ristow and Ruhl, 1994; de Hoop, 1996; Huang and Wu, 1996; Thomson, 1999; Biondi, 2002).

However, migration by downward continuation imposes limitations on the dip of reflectors that can be imaged since it favors energy which is propagating mainly in the downward direction. Upward propagating energy, e.g., overturning waves, can be imaged in principle using downward continuation methods (Hale et al., 1992), although the procedure is difficult, particularly for prestack data. In contrast, Kirchhoff-type methods based on ray-traced traveltimes can image steep dips and handle overturning waves, although those methods are far less reliable in complex environments given their high-frequency asymptotic nature.

The steep-dip limitation of downward continuation techniques has been addressed in several ways:

- A first option is to increase the angular accuracy of the extrapolation operator, for example by employing methods from the Fourier finite-difference (FFD) family (Ristow and Ruhl, 1994; Biondi, 2002), or the Generalized Screen Propagator (GSP) family (de Hoop, 1996; Huang and Wu, 1996). The enhancements brought about by these methods come at a price, since they increase the cost of extrapolation without guaranteeing unconditional stability.

- A second option is to perform the wavefield extrapolation in tilted coordinate systems (Etgen, 2002), or by designing sources which favor illumination of particular regions of the image (Rietveld and Berkhout, 1994; Chen et al., 2002). We can thus increase angular accuracy, although those methods are best suited for a subset of the model (a salt flank, for example), while potentially decreasing the accuracy in other regions. In complex models it is also not obvious what is an optimal tilt angle for the extrapolation grid.

- A third possibility is hybridization of wavefield and ray-based techniques, either in the form of Gaussian beams (Červený, 2001; Hill, 2001; Gray et al., 2002), coherent states (Albertin et al., 2001), or beam-waves (Brandsberg-Dahl and Etgen, 2003). Such techniques are quite powerful, since they couple wavefield methods with multipathing and band-limited properties, with ray methods, which deliver arbitrary directions of propagation, even overturning. The main strength of those techniques, is also their main weakness, i.e. they are formulated in terms of decoupled beams. Beams may leave shadow zones in various parts of the model, which hamper their imaging abilities. Furthermore, beams have limited size, which in turn limits the extent of the diffractions created by sharp features in the model to that of any particular beam, no matter how accurate the extrapolator within each beam is. In addition, the narrow extrapolation domain poses serious beam superposition problems, such as beam boundary effects.

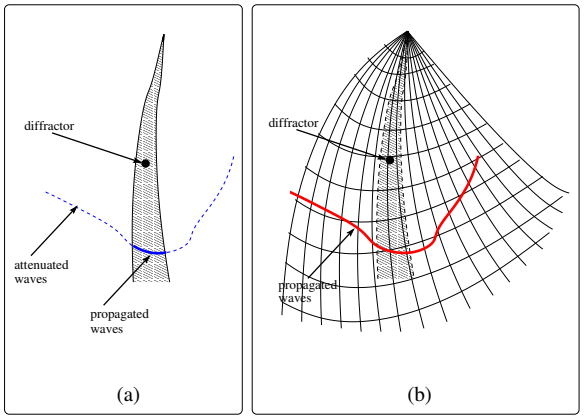

Figure 1: The extrapolated energy is attenuated at beam boundaries (a), but is propagated in a Riemmanian coordinate system (b).

The main idea of our paper is to couple the beams together and extrapolate within all of them at once. Therefore, we cannot talk about beams anymore, but instead we need to talk about continuously changing coordinate systems. We extend downward continuation in a regular Cartesian space to wavefield extrapolation in distorted coordinates, known in differential geometry as *Riemannian spaces*, thus the name of our method. We formulate the theory in arbitrary 3-D semi-orthogonal Riemannian spaces, e.g., ray coordinates, although those coordinate systems do not necessarily need to have a physical meaning as long as they fulfill the semi-orthogonality condition. Examples of such coordinate systems include, but are not limited to, fans of rays emerging from a source point, or bundles of rays initiated by plane waves of arbitrary initial dips at the source. The ray coordinate system can also be created on the fly using an adaptive procedure, as described by Shragge and Sava (2004). A special case of our method is represented by extrapolation in polar/spherical coordinates (Nichols, 1994).

Our method represents a finite-difference solution to the acoustic wave-equation in ray coordinates. In this respect, it is related to Huygens wavefront tracing (Sava and Fomel, 2001), which is a finite-difference solution to the eikonal equation in ray coordinates.

The upside of our method is that the coordinate system may follow

the waves, and can even overturn, such that we can use one-way extrapolators to image diving waves. We can also use extrapolators with small angle accuracy (e.g. 15°), since, in principle, we are never too far from the actual direction in which waves propagate. We are also not confined to the extent of any individual beam, therefore we can track diffractions for their entire spatial extent (Figure 1).

ACOUSTIC WAVE-EQUATION

The Laplacian operator of a scalar function $\mathcal{U}$ in an arbitrary Riemannian space with coordinates $\{\xi_1,\xi_2,\xi_3\}$ has the form

$$\Delta\mathcal{U}=\sum_{i=1}^{3}\frac{1}{\sqrt{|\mathbf{g}|}}\frac{\partial}{\partial\xi_i}\left(\sum_{j=1}^{3}g^{ij}\sqrt{|\mathbf{g}|}\,\frac{\partial\mathcal{U}}{\partial\xi_j}\right), \tag{1}$$

where g^{ij} is a component of the associated metric tensor, and $|\mathbf{g}|$ is its determinant (Synge and Schild, 1978).

The expression simplifies if one of the coordinates (e.g. the coordinate of one-way wave extrapolation) is orthogonal to the other coordinates. Let $\xi_1=\xi$, $\xi_2=\eta$, and $\xi_3=\zeta$, with ζ orthogonal to both ξ and η. Then the metric tensor has the matrix

$$\left[g_{ij}\right]=\begin{bmatrix}E & F & 0\\ F & G & 0\\ 0 & 0 & \alpha^2\end{bmatrix}, \tag{2}$$

where E, F, G, and α are differential forms that can be found from mapping Cartesian coordinates $\mathbf{x}$ to the general coordinates $\{\xi,\eta,\zeta\}$, as follows: $E=\mathbf{x}_\xi\cdot\mathbf{x}_\xi$, $F=\mathbf{x}_\xi\cdot\mathbf{x}_\eta$, $G=\mathbf{x}_\eta\cdot\mathbf{x}_\eta$, and $\alpha^2=\mathbf{x}_\zeta\cdot\mathbf{x}_\zeta$. The associated metric tensor has the matrix

$$\left[g^{ij}\right]=\begin{bmatrix}+G/J^2 & -F/J^2 & 0\\ -F/J^2 & +E/J^2 & 0\\ 0 & 0 & 1/\alpha^2\end{bmatrix}, \tag{3}$$

where $J^2=EG-F^2$. The metric determinant takes the form $|\mathbf{g}|=\alpha^2J^2$. Thus, the Helmholtz wave equation for propagating waves in a 3-D Riemannian space becomes:

$$\frac{1}{\alpha J}\left[\frac{\partial}{\partial\zeta}\left(\frac{J}{\alpha}\frac{\partial\mathcal{U}}{\partial\zeta}\right)+\frac{\partial}{\partial\xi}\left(G\frac{\alpha}{J}\frac{\partial\mathcal{U}}{\partial\xi}-F\frac{\alpha}{J}\frac{\partial\mathcal{U}}{\partial\eta}\right)+\frac{\partial}{\partial\eta}\left(E\frac{\alpha}{J}\frac{\partial\mathcal{U}}{\partial\eta}-F\frac{\alpha}{J}\frac{\partial\mathcal{U}}{\partial\xi}\right)\right]=-\frac{\omega^2}{v^2}\mathcal{U}\,. \tag{4}$$

In equation (4), ω is temporal frequency, $v[\mathbf{x}(\xi,\eta,\zeta)]$ is the wave propagation velocity, and $\mathcal{U}$ represents a propagating wave.

ONE-WAY WAVE-EQUATION

Equation (4) can be used to describe two-way propagation of acoustic waves in a semi-orthogonal Riemannian space. For one-way wavefield extrapolation, we need to modify the acoustic wave equation (4) by selecting a single direction of propagation.

In order to simplify the computations, we introduce the notations: $c_{\zeta\zeta}=\frac{1}{\alpha^2}$, $c_{\xi\xi}=\frac{G}{J^2}$, $c_{\eta\eta}=\frac{E}{J^2}$, $c_{\xi\eta}=\frac{F}{J^2}$, $c_\zeta=\frac{1}{\alpha J}\frac{\partial}{\partial\zeta}\left(\frac{J}{\alpha}\right)$, $c_\xi=\frac{1}{\alpha J}\left[\frac{\partial}{\partial\xi}\left(G\frac{\alpha}{J}\right)-\frac{\partial}{\partial\eta}\left(F\frac{\alpha}{J}\right)\right]$, and $c_\eta=\frac{1}{\alpha J}\left[\frac{\partial}{\partial\eta}\left(E\frac{\alpha}{J}\right)-\frac{\partial}{\partial\xi}\left(F\frac{\alpha}{J}\right)\right]$. All these quantities can be computed by finite-differences for any choice of a Riemannian coordinate system which fulfills the orthogonality condition indicated earlier. In particular, we can use ray coordinates to compute those coefficients. With these notations, the dispersion relation for the wave-equation in a semi-orthogonal 3-D Riemannian space is:

$$-c_{\zeta\zeta}k_\zeta^2-c_{\xi\xi}k_\xi^2-c_{\eta\eta}k_\eta^2+ic_\zeta k_\zeta+ic_\xi k_\xi+ic_\eta k_\eta-c_{\xi\eta}k_\xi k_\eta=-\omega^2s^2\,. \tag{5}$$

For one-way wavefield extrapolation, we need to solve the second order equation (5) for the wavenumber of the extrapolation direction k_ζ, and select the solution with the appropriate sign to extrapolate waves in the desired direction:

$$k_\zeta=i\frac{c_\zeta}{2c_{\zeta\zeta}}\pm\sqrt{\frac{(\omega s)^2}{c_{\zeta\zeta}}-\left(\frac{c_\zeta}{2c_{\zeta\zeta}}\right)^2-\sum_{j=\xi,\eta}\left[\frac{c_{jj}}{c_{\zeta\zeta}}k_j^2-i\frac{c_j}{c_{\zeta\zeta}}k_j\right]-\frac{c_{\xi\eta}}{c_{\zeta\zeta}}k_\xi k_\eta}\,. \tag{6}$$

The solution with the positive sign in equation (6) corresponds to propagation in the positive direction of the extrapolation axis ζ.

We note that the coordinate system coefficients for Riemannian wavefield extrapolation (c) have singularities at caustics, e.g., when the geometrical spreading term J, defining a cross-sectional area of a ray tube, goes to zero. In our examples, we have used simple numerical regularization, by adding a small non-zero quantity to the denominators to avoid division by zero.

A solution to the one-way wave-equation is represented by pure finite-difference methods in the $\omega-x$ domain, which can be implemented either as implicit (Claerbout, 1985), or as explicit methods (Hale, 1991). For the same stencil size, the implicit methods are more accurate and robust than explicit methods, although harder to implement, particularly in 3-D. However, explicit methods of comparable accuracy can be designed using larger stencils.

For the implicit methods, various approximations to the square root in equation (6) lead to approximate equations of various orders of accuracy. In the Cartesian space, those methods are known by their respective angular accuracy as the 15° equation, 45° equation and so on. Although the meanings of 15°, 45° are undefined in Riemannian coordinates, we can still write approximations for the numerical finite-difference solutions using analogous approximations.

A simple way of deriving the 15° equation is by a second order Taylor series expansion of the extrapolation wavenumber k_ζ relative to k_ξ and k_η:

$$k_\zeta\left(k_\xi,k_\eta\right)\approx k_\zeta\left(k_\xi=0,k_\eta=0\right)+\left.\frac{\partial k_\zeta}{\partial k_\xi}\right|_0k_\xi+\left.\frac{\partial k_\zeta}{\partial k_\eta}\right|_0k_\eta+\\+\frac{1}{2}\left.\frac{\partial^2k_\zeta}{\partial k_\xi^2}\right|_0k_\xi^2+\left.\frac{\partial^2k_\zeta}{\partial k_\xi\,\partial k_\eta}\right|_0k_\xi k_\eta+\frac{1}{2}\left.\frac{\partial^2k_\zeta}{\partial k_\eta^2}\right|_0k_\eta^2\,. \tag{7}$$

If we plug equation (6) into equation (7), we obtain the 15° equation in a semi-orthogonal 3-D Riemannian space:

$$k_\zeta\approx i\frac{c_\zeta}{2c_{\zeta\zeta}}+k_o+\frac{1}{2\,k_o}\left[\frac{c_\xi c_\eta}{2c_{\zeta\zeta}^2\,k_o^2}-\frac{c_{\xi\eta}}{c_{\zeta\zeta}}\right]k_\xi k_\eta+\\+\sum_{j=\xi,\eta}\left[\frac{ic_j}{2c_{\zeta\zeta}\,k_o}k_j+\frac{1}{2\,k_o}\left[\left(\frac{c_j}{2c_{\zeta\zeta}\,k_o}\right)^2-\frac{c_{jj}}{c_{\zeta\zeta}}\right]k_j^2\right], \tag{8}$$

where $k_o^2=\frac{(\omega s)^2}{c_{\zeta\zeta}}-\left(\frac{c_\zeta}{2c_{\zeta\zeta}}\right)^2$.

EXAMPLES

We illustrate our method with several synthetic examples of various degrees of complexity. In all examples, we use extrapolation in 2-D orthogonal Riemannian spaces (ray coordinates), and compare the results with extrapolation in Cartesian coordinates. We present

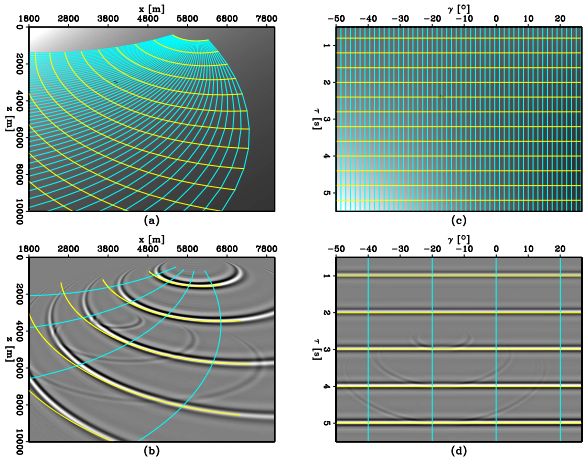

Figure 2: Simple linear gradient model: Cartesian coordinates (a,b) and ray coordinates (c,d). velocity model with an overlay of the ray coordinate system initiated by a point source at the surface (a); image obtained by downward continuation in Cartesian coordinates with the 15° equation (b); velocity model with an overlay of the ray coordinate system (c); image obtained by wavefield extrapolation in ray coordinates with the 15° equation (d).

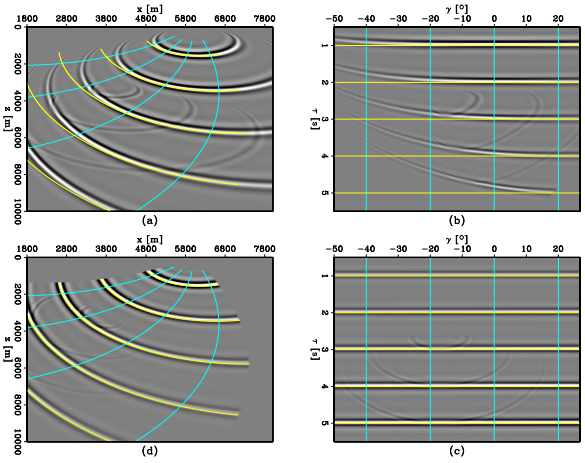

Figure 3: Simple linear gradient model: the image obtained by downward continuation in Cartesian coordinates with the 15° equation (a); the image in panel (a) interpolated to ray coordinates (b); image obtained by extrapolation in ray coordinates with the 15° equation (c); the image in panel (c) interpolated to Cartesian coordinates (d).

images obtained by migration of synthetic datasets represented by events equally spaced in time. In all examples, (x,z) are Cartesian coordinates, and (τ,γ) are ray coordinates for point sources. γ stands for shooting angle, and τ for one-way traveltime.

Our first example is designed to illustrate our method in a fairly simple model. We use a 2-D model with horizontal and vertical gradients $v(x,z) = 250 + 0.2\ x + 0.15\ z$ m/s which gives waves propagating from a point source a pronounced tendency to overturn (Figure 2). The model also contains a diffractor located around $x = 3800$ m and $z = 3000$ m.

We use ray tracing to create an orthogonal ray coordinate system corresponding to a point source on the surface at $x = 6000$ m. Figure 2(a) shows the velocity model and the rays in the original Cartesian coordinate system (x,z). Figure 2(c) shows the velocity model mapped into the ray coordinate system (τ,γ). The diffractor is mapped to $\tau = 2.4$ s and $\gamma = -18°$ measured from the vertical. The synthetic data we use is represented by impulses at equal intervals. In ray coordinates, this source is represented by a plane-wave evenly distributed over all shooting angles γ.

Figure 2(b) shows the image obtained by downward continuation in Cartesian coordinates using the standard 15° equation. Figure 2(d) shows the image obtained by wavefield extrapolation in ray coordinates using the equivalent 15° equation. The overlays in panels (b) and (d) are wavefronts at every 1.0 s and rays shot at every 20° for comparison between the images in ray and Cartesian coordinates.

Figure 3 is a direct comparison of the results obtained by extrapolation in the two coordinate systems. The image created by extrapolation in Cartesian coordinates (a) is mapped to ray coordinates (b). The image created by extrapolation in ray coordinates (c) is mapped to Cartesian coordinates (d). Since we use the same velocity for ray tracing and for wavefield extrapolation, we expect the wavefields and the overlain wavefronts to be in agreement. The most obvious mismatch occurs in regions where the 15° equation fails to extrapolate correctly at steep dips (around $\gamma = (-20,-50)°$. This is not surprising since, as its name indicates, this equation is only accurate up to 15°. However, this limitation is eliminated in ray coordinates, because the coordinate system brings the extrapolator in a reasonable position and at a good angle, although the extrapolator uses an equation of a similar order of accuracy.

Another interesting observation in Figures 3 (a) and (d) concerns the diffractor we introduced in the velocity model. When we extrapolate in Cartesian coordinates, the diffraction is only accurate to a small angle relative to the extrapolation direction (vertical). In contrast, the diffraction develops relative to the propagation direction when computed in ray coordinates, thus being more accurate after mapping to Cartesian coordinates. We can also observe that the diffractions created by the anomaly in the velocity model are not at all limited in the ray coordinates domain. In a beam-type approach, such diffraction would not develop beyond the extent of any particular beam which interacts with it. Neighboring beams would be insensitive to the presence of the velocity anomaly.

Our next example concerns the more complicated Marmousi model. Figure 4 shows the velocity models mapped into the two different domains, and the wavefields obtained by extrapolation in each one of them. We create the ray coordinate system by ray tracing in a smooth version of the model, and extrapolate in the rough version. The source is located on the surface at $x = 5000$ m.

In this example, the wavefields triplicate in both domains (Figure 5). Since we are using a 15° equation, extrapolation in Cartesian coordinates is only accurate for the small incidence angles, as can be seen in panels (a) and (b). In contrast, extrapolating in ray coordinates (c) does not have the same angle limitation, which can also be seen after mapping back to Cartesian coordinates (d).

CONCLUSIONS

We extend one-way wavefield extrapolation to Riemannian spaces which are, by definition, described by non-orthogonal curvilinear coordinate systems. We choose semi-orthogonal Riemannian coordinates which include, but are not limited to, ray coordinate systems. We define an acoustic wave-equation for semi-orthogonal Riemannian coordinates, from which we derive a one-way wavefield extrapolation equation. We use ray coordinates initiated either

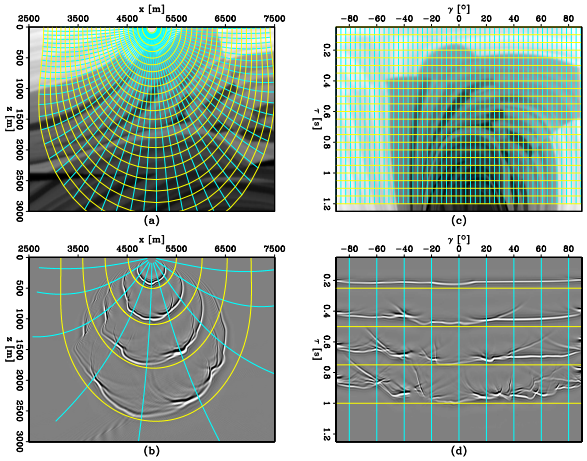

Figure 4: Marmousi model: Cartesian coordinates (a,b) and ray coordinates (c,d). velocity model with an overlay of the ray coordinate system initiated by a point source at the surface (a); image obtained by downward continuation in Cartesian coordinates with the 15° equation (b); velocity model with an overlay of the ray coordinate system (c); image obtained by wavefield extrapolation in ray coordinates with the 15° equation (d).

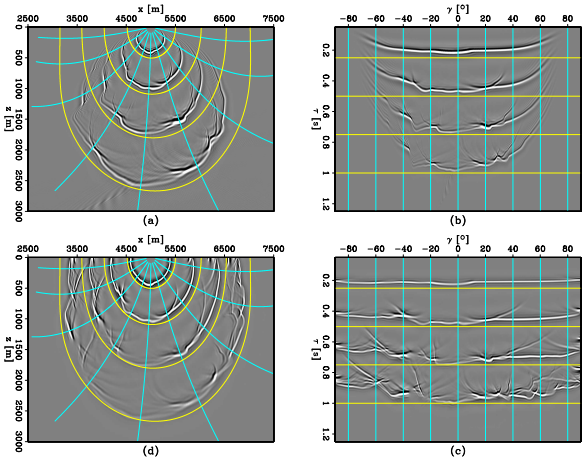

Figure 5: Marmousi model: the image obtained by downward continuation in Cartesian coordinates with the 15° equation (a); the image in panel (a) interpolated to ray coordinates (b); image obtained by extrapolation in ray coordinates with the 15° equation (c); the image in panel (c) interpolated to Cartesian coordinates (d).

from a point source, or from an incident plane wave at the surface. Many other types of coordinates are acceptable, as long as they fulfill the semi-orthogonal condition of our acoustic wave equation.

Since wavefield propagation happens mostly along the extrapolation direction, we can use inexpensive 15° finite-difference or mixed-domain extrapolators to achieve high angle accuracy. If the ray coordinate system overturns, our method can be used to image overturning waves with one-way wavefield extrapolation. Two main applications of our method are imaging of steeply dipping or overturning reflections.

REFERENCES

Albertin, U., Yingst, D., and Jaramillo, H., 2001, Comparing common-offset Maslov, Gaussian beam, and coherent state migrations *in* Expanded Abstracts. Soc. of Expl. Geophys., 913–916.

Biondi, B., 2002, Stable wide-angle Fourier finite-difference downward extrapolation of 3-D wavefields: Geophysics, **67**, 872–882.

Brandsberg-Dahl, S., and Etgen, J., 2003, Beam-wave imaging *in* Expanded Abstracts. Soc. of Expl. Geophys., 977–980.

Chen, L., Chen, Y., and Wu, R., 2002, Target-oriented prestack beamlet migration using Gabor-Daubechies frames *in* Expanded Abstracts. Soc. of Expl. Geophys., 1356–1359.

Claerbout, J. F., 1985, Imaging the Earth's Interior: Blackwell Scientific Publications.

Etgen, J., 2002, Waves, beams and dimensions: an illuminating if incoherent view of the future of migration Soc. of Expl. Geophys.

Gray, S., Notfors, C., and Bleistein, N., 2002, Imaging using multi-arrivals: Gaussian beams or multi-arrival Kirchhoff? *in* Expanded Abstracts. Soc. of Expl. Geophys., 1117–1120.

Hale, D., 1991, Stable explicit depth extrapolation of seismic wavefields: Geophysics, **56**, 1770–1777.

Hale, D., Hill, N. R., and Stefani, J., 1992, Imaging salt with turning seismic waves: Geophysics, **57**, 1453–1462.

Hill, N. R., 2001, Prestack Gaussian-beam depth migration: Geophysics, **66**, 1240–1250.

de Hoop, M. V., 1996, Generalization of the Bremmer coupling series *in* J. Math. Phys. 3246–3282.

Huang, L. Y., and Wu, R. S., 1996, Prestack depth migration with acoustic screen propagators *in* 66th Ann. Internat. Mtg. Soc. of Expl. Geophys., 415–418.

Nichols, D. E., 1994, Imaging complex structures using band-limited Green's functions: Ph.D. thesis, Stanford University. URL `http://sepwww.stanford.edu/public/docs/sep81/index.html`.

Rietveld, W. E. A., and Berkhout, A. J., 1994, Prestack depth migration by means of controlled illumination: Geophysics, **59**, 801–809.

Ristow, D., and Ruhl, T., 1994, Fourier finite-difference migration: Geophysics, **59**, 1882–1893.

Sava, P., and Fomel, S., 2001, 3-D traveltime computation using Huygens wavefront tracing: Geophysics, **66**, 883–889.

Shragge, J., and Sava, P., 2004, Adaptive phase-ray wavefield extrapolation *in* Expanded Abstracts. Soc. of Expl. Geophys.

Synge, J. L., and Schild, A., 1978, Tensor Calculus: Dover.

Thomson, T., 1999, The gap between seismic ray theory and full wavefield extrapolation: Geophys. J. Int, **137**, 364–380.

Červený, V., 2001, Seismic ray theory: Cambridge Univ. Press.